Constraining nonstandard interactions in $\nu_e e$ or $\bar{\nu}_e e$ scattering

J. Barranco* and O. G. Miranda†

Departamento de Física, Centro de Investigación y de Estudios Avanzados del IPN, Apartado Postal 14-740, 07000 México, DF, México

C. A. Moura‡ and J. W. F. Valle§

AHEP Group, Instituto de Física Corpuscular–C.S.I.C./Universitat de València, Edificio Institutos de Paterna, Apartado de Correos 22085, E-46071 Valencia, Spain

(Received 2 February 2006; revised manuscript received 17 May 2006; published 8 June 2006)

We present a new analysis of nonuniversal and flavor changing nonstandard neutrino interactions (NSI) in $\nu_e e$ or $\bar{\nu}_e e$ scattering. Our global analysis of these processes includes all relevant experiments, such as the most recent MUNU measurement from reactor neutrinos, both in the context of the standard model as well as extensions where NSI are present. We also compare our constraints on nonuniversal and flavor changing NSI with results from previous analyses. We stress the importance of combining neutrino and antineutrino data in the resulting constraints on electroweak parameters, and the important role that future low-energy solar neutrino experiments can play in improving existing sensitivities.

DOI: 10.1103/PhysRevD.73.113001 PACS numbers: 13.15.+g, 12.20.Fv, 14.60.St

I. INTRODUCTION

Electron-neutrino and electron-antineutrino scattering off electrons have played an important role in the searches for neutrino oscillations. First hinted by the data from solar and atmospheric neutrinos, oscillations have subsequently been confirmed with reactor and accelerator data [1–3]. Altogether, these experiments now give clear evidence that neutrinos are massive [4] and, therefore, expected to be endowed with nonstandard interactions that may violate leptonic flavor and/or break weak universality [5]. Future experiments, such as BOREXINO [6], aim to use the same reaction for detecting lower energy solar neutrinos. The standard model cross section for this process has been known since the 1970s [7–9], when the first measurements have been carried out [10]. Radiative corrections have been calculated more recently in [11] and there have been recent experiments [12,13]. Currently, there are many proposals to perform new experiments either at relatively high energies [14], in order to test the NuTeV anomaly [15], as well as at low energies [16–19], motivated by the search for a possible nonzero transition neutrino magnetic moment [20].

As already mentioned, it has been long noticed that massive neutrinos are expected to have nonstandard interactions that may arise either from the structure of the charged and neutral current weak interactions in seesaw-type models [5]. Alternatively, they could arise from the exchange of scalar bosons, as present in radiative and/or supersymmetric models of neutrino mass [21,22]. The strength of the expected NSI depends strongly on the model. Here we adopt a model independent approach of simply analyzing their phenomenological implications in neutrino electron scattering. For previous recent studies, see Refs. [23–25].

This possibility has been revived recently as it was noted that both solar and atmospheric neutrino data are consistent with sizable values of the NSI parameters [26–28]. For the case of neutrino interactions with the down-quark, it has been shown that the presence of NSI brings in an ambiguous determination of the solar neutrino oscillation parameters, with a new solution in the so-called "dark side" (with $\sin^2\theta_{\rm sol} \simeq 0.7$ [29]), degenerate with the conventional one, even after taking into account data from the KamLAND experiment. For the case of $\nu_e e^-$ NSI the couplings are also allowed to be large [27].

In this work we concentrate on the detailed study of $\nu_e e^-$ and $\bar{\nu}_e e$ scattering in the presence of nonstandard neutrino interactions, which cannot be found in previous studies, e.g. Refs. [23,25].

We focus on short baseline terrestrial experiments such as the LSND $\nu_e e^-$ scattering and a variety of $\bar{\nu}_e e$ scattering experiments using reactor neutrinos, exploiting their complementarity. Our analysis is new in two ways. First, we relax the conditions under which the constraints on weak couplings have been previously derived. Second, we update the study through the inclusion of more recent data, such as the recent data from the MUNU experiment [30]. Also for completeness, we include the results from the Rovno reactor [31]. Moreover, the results from the Irvine [10] experiment will be analyzed considering the two energy bins that were reported in the original article.

This paper is organized as follows: in Sec. II we recall the basics of $\nu_e e$ scattering in the context of the standard model, in Sec. III we analyze the role of nonstandard

*Electronic address: jbarranc@fis.cinvestav.mx
†Electronic address: Omar.Miranda@fis.cinvestav.mx
‡Electronic address: Celio.Moura@ific.uv.es
§Electronic address: valle@ific.uv.es

neutrino interactions, and in Sec. IV we discuss prospects for further improvements, stressing the role of future low-energy experiments using solar neutrino, as well as experiments using radioactive neutrino sources.

II. THE NEUTRINO ELECTRON SCATTERING

As a warm-up exercise, before considering the case of nonstandard neutrino interactions, let us briefly consider the restrictions placed by current experiments within the context of the standard model.

A. Preliminaries

In the standard model the $\nu_e e$ differential cross section scattering involves both neutral and charged currents and is well known [7] to be

$$\frac{d\sigma}{dT} = \frac{2G_F m_e}{\pi}\left[g_L^2 + g_R^2\left(1 - \frac{T}{E_\nu}\right)^2 - g_L g_R \frac{m_e T}{E_\nu^2}\right], \quad (1)$$

where $G_F = 1.666 \times 10^{-5}$ GeV^2, m_e is the electron mass, T is the kinetic energy of the recoil electron and E_ν is the neutrino energy.

One can see explicitly that the differential cross section in Eq. (1) has a symmetry under the simultaneous transformation $g_L \to -g_L$ and $g_R \to -g_R$. Apart from the last term, it is also invariant under separate sign changes in $g_{L,R}$. For the case of $\bar{\nu}_e e$ scattering one has to exchange g_L by g_R.

For a fixed neutrino energy, the determination of the weak coupling constants $g_L - g_R$, is ambiguous since the same cross section in Eq. (1) is achieved for any $g_L - g_R$ values in an ellipse with one axis given by 1 and the other one by $(1 - \frac{T}{E_\nu})$. However, measurements at different neutrino energies can potentially lift this degeneracy, due to the last term in Eq. (1). For example, for sufficiently low energies, comparable to the electron mass, the extra term rotates the ellipse by a sizable angle

$$\tan 2\theta = \frac{m_e}{(2E_\nu - T)}. \quad (2)$$

On the other hand, the antineutrino cross section defines another ellipse which is perpendicular to the one corresponding to the neutrino case, since the axis width of this ellipse is exactly opposite ($g_L \leftrightarrow g_R$). Therefore, by judicious combinations of energies and/or adding antineutrino data, one expects to lift the above degeneracy, as we will see in the next subsection.

Within the standard model the coupling constants g_L and g_R are expressed, at tree level, as

$$g_L = \tfrac{1}{2} + \sin^2\theta_W \quad (3)$$

$$g_R = \sin^2\theta_W, \quad (4)$$

where $g_L \equiv 1 + g_L^{\rm SM}$, $g_L^{\rm SM}$ being the conventional SM definition. We have checked explicitly that for the present accuracy of the experiments, the above simple formulae are sufficient, as there is no sensitivity to the corresponding radiative corrections given in [11].

B. Analysis

In our global analysis of the $\nu_e e$ and $\bar{\nu}_e e$ scattering we have included all current experiments, namely, the data from the LSND measurement of the neutrino electron scattering cross section [12]; for the antineutrino electron scattering we have considered the two bins measured in the Irvine experiment [10], the results of the Rovno experiment [31] and the more recent result from the MUNU experiment [30]. The experimental results are summarized in Table I.

In order to perform the analysis we need the total cross section which, for the antineutrino case we express as

$$\sigma = \int dT' \int dT \int dE_\nu \frac{d\sigma}{dT}\lambda(E_\nu)R(T, T'), \quad (5)$$

where both spectra and the detector energy resolution function, should be convoluted with the cross sections given in Eq. (1).

In particular for the most recent MUNU measurement from reactor neutrinos [30], we use an antineutrino energy spectrum given by

$$\lambda(E_n u) = \sum_{k=1}^{4} a_k \lambda_k(E_\nu), \quad (6)$$

where a_k is the abundance of ^{235}U ($k = 1$), ^{239}Pu ($k = 2$), ^{241}Pu ($k = 3$) and ^{238}U ($k = 4$) in the reactor, $\lambda_k(E_\nu)$ is the corresponding neutrino energy spectrum which we take from the parametrization given in [32], with the appropri-

TABLE I. Current experimental data on (anti)neutrino electron scattering.

Experiment	Energy range (MeV)	Events	Measurement
LSND $\nu_e e$	10–50	191	$\sigma = [10.1 \pm 1.5] \times E_{\nu_e}(\mathrm{MeV}) \times 10^{-45}$ cm^2
Irvine $\bar{\nu}_e - e$	1.5–3.0	381	$\sigma = [0.86 \pm 0.25] \times \sigma_{V-A}$
Irvine $\bar{\nu}_e - e$	3.0–4.5	77	$\sigma = [1.7 \pm 0.44] \times \sigma_{V-A}$
Rovno $\bar{\nu}_e - e$	0.6–2.0	41	$\sigma = (1.26 \pm 0.62) \times 10^{-44}$ cm^2/fission
MUNU $\bar{\nu}_e - e$	0.7–2.0	68	1.07 ± 0.34 events day^{-1}

ate fuel composition. For energies below 2 MeV there are only theoretical calculations for the antineutrino spectrum which we take from Ref. [33]. For the case of the Irvine experiment we prefer to use the neutrino energy spectrum used by the experimentalists at that time [34].

Regarding the detector resolution function $R(T, T')$ for the case of MUNU it was found to be 8% scaling with the power 0.7 of the energy [30]. For the other two antineutrino experiments included in our analysis the resolution function was not reported, so we neglect resolution effects.

For the LSND electron neutrino experiment we use the theoretical expectation for the total neutrino electron cross section, which is

$$\sigma(\nu_e e) = \frac{2m_e G_F^2 E_\nu}{\pi}\left[g_L^2 + \frac{1}{3}g_R^2\right]. \quad (7)$$

Notice that in this case the term $g_L g_R$ can be neglected, since this experiment was done at high energies of tens of MeV. As a result there is no tilt in the ellipse, as discussed in the previous section (see also Fig. 1).

With this information we proceed to our χ^2 analysis. Altogether, we will have five observables, and therefore, it will be possible to constrain up to four parameters simultaneously. We neglect correlations between experiments; this is a good approximation as the only possible correlation comes from the reactor neutrino energy spectrum, estimated to be less than 2% [32], small in view of the statistical errors. Therefore we can define the χ^2 simply as

$$\chi^2 = \sum_i \frac{(\sigma_i^{\text{theo}} - \sigma_i^{\text{exp}})^2}{\Delta_i^2}, \quad (8)$$

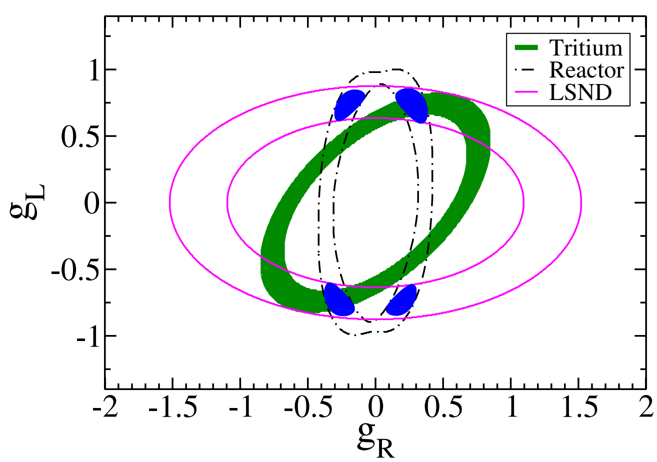

FIG. 1 (color online). Allowed 90% C.L. regions for g_L and g_R obtained by a global fit to neutrino and antineutrino electron scattering data. It is possible to see the existence of four allowed regions. The plot also shows the contribution from LSND neutrino electron scattering (horizontal ellipse) and combined data from reactor experiments (vertical ellipse). The tilted ellipse illustrates the potential of a future low-energy artificial neutrino source (tritium proposal in Ref. [17]).

where the σ_i^{exp} are given by the measurements shown in Table I and Δ_i are the corresponding errors, while σ_i^{theo} is the theoretical expectation.

C. The standard model parameters

In this section we present the results of our fit first in terms of the g_L and g_R coupling constants and, later, we will obtain the value of the standard model weak mixing angle.

To obtain the allowed regions for the g_L and g_R coupling constants we perform a χ^2 analysis as discussed in the previous subsection. These two parameters are determined by five measurements and therefore we will have 3 degrees of freedom. The minimun χ^2 for this case was 0.52.

The results are illustrated in Fig. (1) for 90% C L ($\Delta\chi^2 = 4.61$). In this case one can clearly notice the existence of four possible regions for these parameters. We overlay in the same figure the corresponding equi-cross section regions for current neutrino and antineutrino experiments, which form two perpendicular ellipses, as expected. The neutrino LSND data gives rise to the horizontal ellipse, while the combined antineutrino data lead to the vertical ellipse and therefore reduce the allowed region by restricting the g_L and g_R values to the intersection of the two. Of the existing experiments the ones giving the main contribution to the constraint are the LSND and the Irvine experiments, due to their higher statistics. A more restrictive analysis from the MUNU experiment might be possible by using its binned data, although this is out of the scope of the present work.

We also show in Fig. (1) the case of a future low-energy neutrino experiment, in which case the ellipse is tilted. To illustrate the potential of future low-energy experiments we consider, for definiteness, the case of the NOSTOS proposal, where antineutrinos come from an intense tritium source with a maximum energy of 18.6 KeV [16]. For this case the antineutrino spectrum for the source is taken as [35]

$$\lambda(E_\nu) = A\frac{x}{1-e^{-x}}(Q + m_e - E_\nu) \times E_\nu^2\sqrt{(Q + m_e - E_\nu)^2 - m_e^2}, \quad (9)$$

where A is a normalization factor, $Q = 18.6$ KeV, m_e is the electron mass, and

$$x = 2\pi\alpha_{\text{e.m.}}\frac{Q + m_e - E_\nu}{\sqrt{(Q + m_e - E_\nu)^2 - m_e^2}}. \quad (10)$$

This spectrum is convoluted with the antineutrino differential cross section. The total number of events is set to be 3500 [17] (for 1 yr of data taking).

We see that there is room for such future low-energy neutrino experiments to provide useful input to resolve the

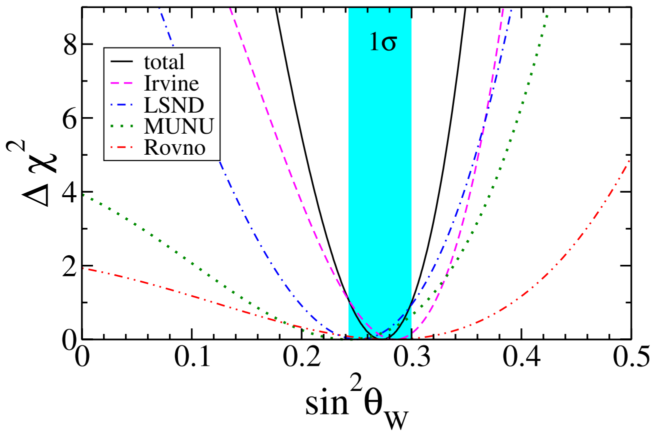

FIG. 2 (color online). $\Delta\chi^2$ for $\sin^2\theta_W$ from $\nu_e e$ or $\bar{\nu}_e e$ scattering. The contribution of each experiment to the $\Delta\chi^2$ is also shown.

current degenerate determination of the weak coupling constants, improving the existing measurements. Unfortunately, as discussed above, the symmetry of the cross section when we make the transformations $g_L \to -g_L$ and $g_R \to -g_R$ can not be lifted by this method. Such a degeneracy is therefore irreducible. This is not an academic ambiguity as it means the validity of the gauge theory description dictated by the standard model. In order to test the future sensitivity we set the experimental measure to be exactly the SM prediction, and we consider only the statistical error. After considering this experimental set up for NOSTOS we obtain the region shown in Fig. 1.

Assuming the validity of the standard model, given by Eqs. (3) our results can also be presented directly in terms of the weak mixing angle. In this case, the combined analysis of the existing (anti)-neutrino-electron scattering experiments gives $\sin^2\theta_W = 0.27 \pm 0.03$. The corresponding minimum for the χ^2 function was $\chi^2_{\rm min} = 0.89$.

The various contributions to $\Delta\chi^2$ from different individual experiments are indicated in Fig. 2. Note that the present fit gives a central value higher than the world average [36], though the error is larger than found in other experiments, because of their small statistics relative to collider experiments. Nevertheless we find this to be interesting as an independent and clean probe of the standard model.

III. NONSTANDARD INTERACTIONS IN $\nu_e e$ AND $\bar{\nu}_e e$ SCATTERING

Solar neutrino data are robust with respect to possible modifications in solar physics involving various types of magnetic fields both in the convective zone [37] as well as radiative zone [38,39]. If present, nonstandard effects are expected to be subleading insofar as providing an explanation of the existing data [40]. However, even taking into account the crucial data from reactor experiments, the current accepted interpretation of solar neutrino data is not yet robust when neutrinos are endowed with nonstandard interactions [29]. In fact it has been shown that the presence of NSI brings in an ambiguous determination of the solar neutrino oscillation parameters, with a new "dark side" solution (with $\sin^2\theta_{\rm sol} \simeq 0.7$ [29]), essentially degenerate with the conventional one. Similarly, despite the good description provided by oscillations of contained and upgoing events which leads to limits on the strength of the NSI strength in a two-neutrino scenario [41], atmospheric neutrino data are still consistent with sizable values of the NSI parameters when three neutrinos are considered [28]. Here we focus on the case of terrestrial experiments involving electron-type neutrinos and antineutrinos.

A. Cross section

A model independent way of introducing such nonstandard interactions is via the effective four fermion Lagrangian [23]

$$-\mathcal{L}^{\rm eff}_{\rm NSI} = \varepsilon^{fP}_{\alpha\beta} 2\sqrt{2} G_F (\bar{\nu}_\alpha \gamma_\rho L \nu_\beta)(\bar{f}\gamma^\rho P f), \quad (11)$$

where f is a first generation SM fermion: e, u or d, and $P = L$ or R, are chiral projectors. With this Lagrangian (11) added to the standard model Lagrangian one can compute the differential cross section for the process $\nu_e e \to \nu_\alpha e$ as

$$\frac{d\sigma(E_\nu, T)}{dT} = \frac{2G_F^2 M_e}{\pi}\Bigg[\Big(\tilde{g}_L^2 + \sum_{\alpha\neq e}|\epsilon^{eL}_{\alpha e}|^2\Big) + \Big(\tilde{g}_R^2 + \sum_{\alpha\neq e}|\epsilon^{eR}_{\alpha e}|^2\Big)\Big(1 - \frac{T}{E_\nu}\Big)^2 - \Big(\tilde{g}_L\tilde{g}_R + \sum_{\alpha\neq e}|\epsilon^{eL}_{\alpha e}||\epsilon^{eR}_{\alpha e}|\Big) m_e \frac{T}{E_\nu^2}\Bigg], \quad (12)$$

with $\tilde{g}_L = g_L + \epsilon^{eL}_{ee}$ and $\tilde{g}_R = g_R + \epsilon^{eR}_{ee}$. This equation has six NSI parameters, two of them correspond to nonuniversal (NU) NSI: ϵ^{eLR}_{ee} and four to flavor changing (FC) NSI: $\epsilon^{eLR}_{e\mu}$ and $\epsilon^{eLR}_{e\tau}$. In view of the stringent (though indirect) constraints on the FC parameters $|\epsilon^{eLR}_{e\mu}| < 7.7 \times 10^{-4}$ [25] we will, for simplicity, neglect FC NSI involvion muon neutrinos. This way we are left with the two NU NSI parameters and two FC parameters, $\epsilon^{eLR}_{e\tau}$.

The agreement between $\nu_e e$ scattering experiments and the standard model predictions had been previously studied in Refs. [23–25] in order to place restrictions on the magnitude of nonstandard interactions. However, existing analyses either restricted the variation of the parameters, which were considered only one-at-a-time [25], or the combination of two NSI parameters (the nonuniversal coupling ϵ^{eR}_{ee} and ϵ^{eR}_{ee}) but using only two experiments [23].

Here we revisit this question generalizing the conditions under which these constraints have been derived and, as we

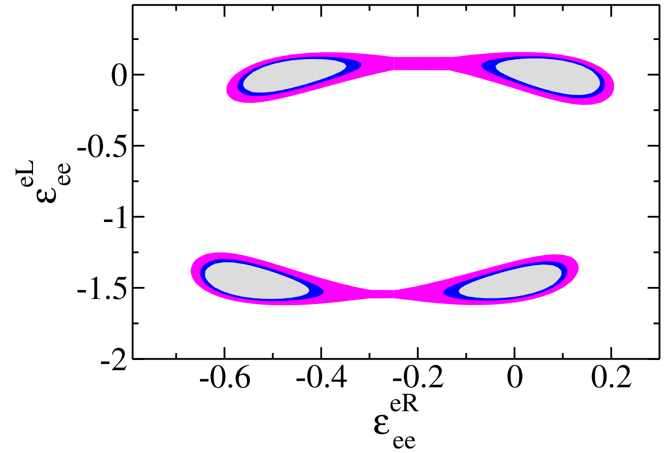

FIG. 3 (color online). Allowed regions at 90, 95, and 99% C.L. for ε_{ee}^{eL} and ε_{ee}^{eR} obtained by a global fit to neutrino and antineutrino electron scattering. The flavor changing NSI parameters were taken equal to zero.

have already mentioned, updating the study through the inclusion of more recent data, such as the data from the MUNU experiment [30]. Also for completeness, we will consider the results from the Rovno reactor [31]. Moreover, the results from the Irvine experiment will be analyzed considering the two energy bins that were reported in the original article.

Although the constraints are expected to be weaker in our case, they will be robust than the ones obtained in the case where the parameters are taken only one-at-a time in the analysis. However, as will be clear at the end of this section, by taking full advantage of the combination of neutrino and antineutrino data we are able to obtain more stringent bounds on "right-handed" NSI parameters than previously.

B. NSI analysis

First we present the results for the case of nonuniversal NSI (ϵ_{ee}^{eL}, ϵ_{ee}^{eR}), with flavor changing parameters set to zero. In Fig. (3) we show the allowed regions at 90, 95 and 99% C L ($\Delta\chi^2 = 4.61, 5.99, 9.21$). The minimum χ^2 was 0.52. One can see that its determination is improved with respect to the current results, although a twofold ambiguity in ϵ_{ee}^{eL} remains. This follows from the discussion given in section , where we stressed that the intersection from the neutrino and antineutrino ellipses (see Fig. 1) does not allow for a unique discrimination of the coupling constant values. It is here that future low-energy experiments have a chance of improving their determination.

The same analysis can be performed for the case where we allow only flavor changing NSI parameters ($\epsilon_{e\tau}^{eL}$, $\epsilon_{e\tau}^{eR}$), or for the general case when we take into account all four parameter simultaneously. The results of this analysis are summarized in Table II. The left column collects previously reported constraints [25], determined under the assumption that only one NSI parameter was allowed to take on nonzero values. In the second column, for comparison, we present the result of our fit for the same case of a one-parameter analysis. The third column gives our result for a two parameters analysis, where only NU or FC parameters are nonzero, therefore the NU region corresponds to the one shown in Fig. 3. Finally, the fourth column shows a more general case when from the four parameters we take a projection over two of them (either NU or FC) allowing the other two to take on nonzero values. In this case for a 90% C L we have again to consider $\Delta\chi^2 = 4.61$ but the regions are wider as can be seen from the table. The minimum χ^2 for this analysis was 0.49.

One can see that the constraints for the case when only one parameter is considered are similar to the results previously reported [25], with the exception of $\epsilon_{e\tau}^{eR}$ and ϵ_{ee}^{eR} where ours are clearly better. This is natural to expect and follows from the fact that we are combining the LSND neutrino electron scattering data with the antineutrino electron scattering data. This allows us to obtain four different regions for the left and right couplings as can also be seen from Fig. (1). It is important to note, however that when the four parameters are taken as freely-varying our constraints are weaker than the existing ones for the case of "left-handed" couplings $\epsilon_{e\tau}^{eL}$ and ϵ_{ee}^{eL}, as expected (in fact they could be as large as order unity). In contrast, for the case of the "right-handed" NSI couplings, our constraints better than the previous limits. The explanation of this puzzle is that, in this case, in contrast to previous work, we combine neutrino and antineutrino data. As we

TABLE II. Constraints on NSI parameters at 90% C.L. In the first column we show the previous constraints obtained in [25], while in the second we show the corresponding results found in the present analysis. The last two columns show the case in which two and four parameters are allowed to vary simultaneously (see the text for explanation).

	Previous limits	One parameter	Two parameters	All parameters
ϵ_{ee}^{eL}	$-0.07 < \epsilon_{ee}^{eL} < 0.11$	$-0.05 < \epsilon_{ee}^{eL} < 0.12$	$-0.13 < \epsilon_{ee}^{eL} < 0.12$	$-1.58 < \epsilon_{ee}^{eL} < 0.12$
ϵ_{ee}^{eR}	$-1.0 < \epsilon_{ee}^{eR} < 0.5$	$-0.04 < \epsilon_{ee}^{eR} < 0.14$	$-0.07 < \epsilon_{ee}^{eR} < 0.15$	$-0.61 < \epsilon_{ee}^{eR} < 0.15$
$\epsilon_{e\tau}^{eL}$	$\lvert\epsilon_{e\tau}^{eL}\rvert < 0.4$	$\lvert\epsilon_{e\tau}^{eL}\rvert < 0.44$	$\lvert\epsilon_{e\tau}^{eL}\rvert < 0.43$	$\lvert\epsilon_{e\tau}^{eL}\rvert < 0.85$
$\epsilon_{e\tau}^{eR}$	$\lvert\epsilon_{e\tau}^{eR}\rvert < 0.7$	$\lvert\epsilon_{e\tau}^{eR}\rvert < 0.27$	$\lvert\epsilon_{e\tau}^{eR}\rvert < 0.31$	$\lvert\epsilon_{e\tau}^{eR}\rvert < 0.38$

have already seen, this has a great impact in constraining the "right-handed" NSI paramneters.

IV. SUMMARY AND PROSPECTS

We have presented a global analysis of nonstandard neutrino interactions in electron (anti)-neutrino scattering off electrons, including all current experiments, such as the most recent MUNU measurement from reactor neutrinos. We have discussed the resulting constraints both in the context of the standard model as well as extensions where nonstandard neutrino interactions are present. We obtained constraints on nonuniversal and flavor changing NSI and compared our bounds with those obtained in previous analyses. We find that substantial room for improvement is expected from $\nu_e e$ or $\bar{\nu}_e e$ low-energy scattering experiments. There are several proposals of this type, either using solar neutrinos, such as BOREXINO [6], or experiments using artificial neutrino sources, such as [19], that will be helpful in constrining NSI parameters as well as for other type of new physics (see for example [42,43]). From the point of view of pinning down the interactions of the ν_e and $\bar{\nu}_e$ low-energy scattering experiments offer an alternative frontier that complements information that comes from higher energies [44,45].

In summary, cross section measurements by themselves, at a given energy, lead to a degeneracy in the coupling constants and, therefore, in the determination of the NSI parameters. This degeneracy can be partially removed by considering both neutrino and antineutrino scattering off electrons. Further improvements require low-energy neutrino experiments.

ACKNOWLEDGMENTS

We thank Nicolao Fornengo for reading the manuscript. This work has been supported by Spanish Grants No. BFM2002-00345 and FPA2005-01269, by Conacyt-México, and by the EC RTN network MRTN-CT-2004-503369. C. A. M. is supported by the AlBan program. J. B. would like to thank IFIC/CSIC for the kind hospitality during the visit where part of this work was done.

[1] Y. Fukuda *et al.* (Super-Kamiokande Collaboration), Phys. Rev. Lett. **81**, 1562 (1998).
[2] Q. R. Ahmad *et al.* (SNO Collaboration), Phys. Rev. Lett. **89**, 011301 (2002).
[3] K. Eguchi *et al.* (KamLAND Collaboration), Phys. Rev. Lett. **90**, 021802 (2003).
[4] For a review, see M. Maltoni, T. Schwetz, M. A. Tortola, and J. W. F. Valle, New J. Phys. **6**, 122 (2004).
[5] J. Schechter and J. W. F. Valle, Phys. Rev. D **22**, 2227 (1980).
[6] G. Alimonti *et al.* (Borexino Collaboration), Astropart. Phys. **16**, 205 (2002).
[7] D. Y. Bardin, S. M. Bilenky, and B. Pontecorvo, Phys. Lett. **32B**, 68 (1970).
[8] G. 't Hooft, Phys. Lett. **37B**, 195 (1971).
[9] H. H. Chen and B. W. Lee, Phys. Rev. D **5**, 1874 (1972).
[10] F. Reines, H. S. Gurr, and H. W. Sobel, Phys. Rev. Lett. **37**, 315 (1976).
[11] J. N. Bahcall, M. Kamionkowski, and A. Sirlin, Phys. Rev. D **51**, 6146 (1995).
[12] L. B. Auerbach *et al.* (LSND Collaboration), Phys. Rev. D **63**, 112001 (2001).
[13] C. Amsler *et al.* (Bugey Collaboration), Phys. Lett. B **545**, 57 (2002).
[14] J. M. Conrad, J. M. Link, and M. H. Shaevitz, Phys. Rev. D **71**, 073013 (2005).
[15] G. P. Zeller *et al.* (NuTeV Collaboration), Phys. Rev. Lett. **88**, 091802 (2002); **90**, 239902(E) (2003)
[16] I. Giomataris and J. D. Vergados, Phys. At. Nucl. **67**, 1097 (2004).
[17] Y. Giomataris and J. D. Vergados, Nucl. Instrum. Methods Phys. Res., Sect. A **530**, 330 (2004).
[18] V. I. Kopeikin, L. A. Mikaelian, and V. V. Sinev, Yad. Fiz. **66**, 736 (2003) [Phys. At. Nucl. **66**, 707 (2003)].
[19] B. S. Neganov *et al.*, Yad. Fiz. **64**, 2033 (2001); [Phys. At. Nucl. **64**, 1948 (2001)].
[20] J. Schechter and J. W. F. Valle, Phys. Rev. D **24**, 1883 (1981); **25**, 283(E) (1982).
[21] A. Zee, Phys. Lett. **93B**, 389 (1980).
[22] K. S. Babu, Phys. Lett. B **203**, 132 (1988).
[23] Z. Berezhiani and A. Rossi, Phys. Lett. B **535**, 207 (2002).
[24] Z. Berezhiani, R. S. Raghavan, and A. Rossi, Nucl. Phys. **B638**, 62 (2002).
[25] S. Davidson, C. Pena-Garay, N. Rius, and A. Santamaria, J. High Energy Phys. 03 (2003) 011.
[26] A. Friedland, C. Lunardini, and C. Pena-Garay, Phys. Lett. B **594**, 347 (2004).
[27] M. M. Guzzo, P. C. de Holanda, and O. L. G. Peres, Phys. Lett. B **591**, 1 (2004).
[28] A. Friedland, C. Lunardini, and M. Maltoni, Phys. Rev. D **70**, 111301 (2004).
[29] O. G. Miranda, M. A. Tortola, and J. W. F. Valle, hep-ph/0406280.
[30] Z. Daraktchieva *et al.* (MUNU Collaboration), Phys. Lett. B **564**, 190 (2003).
[31] A. I. Derbin *et al.*, JETP Lett. **57**, 768 (1993).
[32] P. Huber and T. Schwetz, Phys. Rev. D **70**, 053011 (2004).
[33] V. I. Kopeikin, L. A. Mikaelyan, and V. V. Sinev, Yad. Fiz. **60**, 172 (1997) [Phys. At. Nucl. **60**, 230 (1997)].
[34] F. T. Avignone III, Phys. Rev. D **2**, 2609 (1970).
[35] A. Ianni, D. Montanino, and G. Scioscia, Eur. Phys. J. C **8**, 609 (1999).
[36] S. Eidelman *et al.* (Particle Data Group), Phys. Lett. B **592**, 1 (2004).

[37] O. G. Miranda, T. I. Rashba, A. I. Rez, and J. W. F. Valle, Phys. Rev. D **70**, 113002 (2004); Phys. Rev. Lett. **93**, 051304 (2004).

[38] C. P. Burgess, N. S. Dzhalilov, T. I. Rashba, V. B. Semikoz, and J. W. F. Valle, Mon. Not. R. Astron. Soc. **348**, 609 (2004).

[39] C. P. Burgess *et al.*, J. Cosmol. Astropart. Phys. 01 (2004) 007.

[40] For a review, see S. Pakvasa and J. W. F. Valle, Proc. Indian Natl. Sci. Acad., Part A 70A, 189 (2004).

[41] N. Fornengo, M. Maltoni, R. Tomas Bayo, and J. W. F. Valle, Phys. Rev. D **65**, 013010 (2002).

[42] I. Barabanov *et al.*, Nucl. Phys. **B546**, 19 (1999).

[43] O. G. Miranda, V. Semikoz, and J. W. F. Valle, Phys. Rev. D **58**, 013007 (1998).

[44] F. Ardellier *et al.*, hep-ex/0405032.

[45] A. de Gouvea and J. Jenkins, hep-ph/0603036 and reference therein.